Impact of Silver Nanoparticles Embedded in a Silica Layer on the Surface Morphology of the Structure: Evaluation by Atomic Force Microscopy

Sariette Nowa-Tatchum, Christina Villeneuve-Faure, Laurent Boudou, Kremena Makasheva

Impact of silver nanoparticles embedded in a silica layer on the surface morphology of the structure: Evaluation by Atomic Force Microscopy

Sariette Nowa-Tatchun, Christina Villeneuve-Faure, *Member, IEEE*,
Laurent Boudou and Kremena Makasheva, *Member, IEEE*

***Abstract*— This work presents a study on the surface morphology of silica-based dielectric structures, homogeneous or nanocomposite, intended to be electrically connected with external circuitry *i.e.,* to receive electrodes on their surface. The evaluation is performed with Atomic Force Microscopy (AFM) and specific attention is paid to the surface waviness, imposed by the presence of silver nanoparticles (AgNPs) embedded very close to the silica layer surface. Such departure from planarity may strongly modify the designed electric field through local enhancements of the applied field (by a factor of 20 or more) and thus, to alter the device performance.**

I. Introduction

Reduction of the size (miniaturization) and decreasing the energy consumption remain main challenges in the conception of many electronic devices like the conventionally developed different types of sensors and micro-commutators, and the newly considered ones like memristors for neuromorphic computing, flexible electronics, micro/nano-robotic manipulation, nano-sized robots, *etc*. [1]–[7] The nanotechnology in general, and the nanocomposite/nanostructured materials in particular, offer motivating ideas for conception of the above mentioned devices. Involvement of different kinds of nanoparticles in the design of the structures allows for achievement of better performances of the devices, like better sensitivity and customizable adaptability. Though, the requirements for stability of operation and reliability of the applied nanocomposite/nanostructured materials are strongly increased, involving control over the material properties at each step of the device assembly.

A critical part of the designed structures is the dielectric material and especially the metal(electrode)/dielectric interfaces where different physical phenomena occur, in particular the dielectric charging phenomenon. When implementing nanocomposite materials in devices the planarity of the layers has some tolerable degrees but depending on the elaboration method (chemical or physical, or a combination of the two) and due to the very small layer thicknesses the surface of nanocomposites may present some irregularities/waviness, especially when the embedded nanoparticles/nanoobjects are positioned in the subsurface or are slightly showing on the surface. Such surface induced situations present challenges for the electrical contacts that connect these materials with external circuitry, since the applied electric field might differs substantially from the designed one due to points where local enhancement may appear and consequently alter the device performance [8], [9].

In this work we present a non-destructive way, based on Atomic Force Microscopy (AFM), to evaluate the surface morphology of different dielectric structures that are intended to be electrically connected *i.e.*, to receive electrodes on their surface: SiO_2 homogeneous layers elaborated by thermal growth on a Si-substrate and plasma deposited ones, as well as nanocomposites containing a plane of silver nanoparticles (AgNPs), embedded very close to the surface in plasma deposited SiO_2 layers. Apart from measurements of the surface roughness, we report on a protocol for evaluation of the surface waviness due to the presence of AgNPs and an assessment of the size of the AgNPs depending on the distance from the silica surface at which they are localized.

II. Experimental part

A. Sample design and synthesis

Thermal silica (SiO_2) layers with thickness around 100 nm were grown on doped Si-substrates (p-type, boron, resistivity ρ_{Si} = 7-13 Ωcm) at 1100°C under well controlled slightly oxidizing atmosphere, using a N_2–O_2 gas mixture containing 1.0% of O_2. This process provides a very good control over the silica homogeneity and the layer thickness.

Homogeneous plasma silica layers were deposited on the same type of Si-substrates in an axially-asymmetric radiofrequency capacitively-coupled discharge sustained at low gas pressure in an argon (Ar)-hexamethyldisiloxane (HMDSO, $Si_2O(CH_3)_6$)-oxygen (O_2) mixture. More details on the plasma process and the conditions for SiO_2 layers deposition can be found elsewhere [10]. The layer thickness was controlled by the deposition time.

The AgNPs-based nanocomposites were synthesized in the same plasma reactor that successfully combines metal sputtering and plasma enhanced chemical vapor deposition. They consist of a plane of AgNPs embedded in silica matrix at a well-controlled depth close to the surface (Fig. 1). This stratified structure was obtained in a three-step process: 1-deposition of SiO_2-base, 2-synthesis of the plane of AgNPs and 3-deposition of the SiO_2-cover layer. The distance at

Research supported by Agence Nationale de la Recherche in France, project ANR BENDIS (ANR-21-CE09-0008).

Christina Villeneuve-Faure (christina.villeneuve@laplace.univ-tlse.fr) and Kremena Makasheva (kremena.makasheva@laplace.univ-tlse.fr) are the corresponding authors. All authors are with LAPLACE (Laboratory on Plasma and Conversion of Energy), Université de Toulouse, CNRS, UT3, INPT, Toulouse, France.

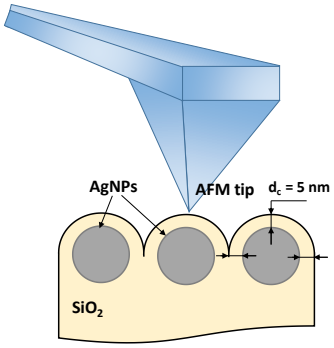

Figure 1. Schematic representation of the AFM tip probing the surface waviness of the AgNPs-based nanocomposite (not at scale).

which the AgNPs were embedded in the silica matrix was controlled by the thickness of the SiO_2-cover layer. The size and density of the AgNPs were varied [10].

Structural characterization of the obtained nanocomposites was achieved by spectroscopic ellipsometry with a Semilab SE-2000 ellipsometer in the 250 – 850 nm spectral range with an incident angle of 75°. Forouhi-Bloomer dispersion law was applied to extract the thickness and the optical properties of the silica layers. Observation of the nanocomposites was performed with Transmission Electron Microscopy (TEM) by a JEOL JEM 2100F microscope.

B. *Characterization by Atomic Force Microscopy*

AFM measurements were performed using a Bruker Multimode 8 apparatus. A silicon AFM tip with curvature radius R_c = 5 nm and spring constant k = 2.4 N/m was used. The surface morphology was probed in tapping mode using a running frequency of 320 kHz. Two different surface areas were investigated using a 384 × 384 measurement point matrix: 10 µm × 10 µm and 1 µm × 1 µm, representing a lower and a higher resolution, respectively. The scan rate was fixed to 0.8 Hz. The amplitude set-point, which controls the interaction force between the tip and the surface, and the Proportional-Integral (PI) gains, which control the response time, were adjusted to limit tip wear and ensure measurements reliability.

The surface roughness is reported here through the arithmetic and quadratic roughness, as obtained according their standard definitions:

$$R_a = \frac{1}{N}\sum_{j=1}^{N}\left|Z_j\right|, \quad R_q = \sqrt{\frac{1}{N}\sum_{j=1}^{N}Z_j^{\,2}}, \tag{1}$$

where Z_j is the height at point j and N is the total number of scanned points *i.e.*, 384 × 384 points.

III. Results and Discussion on the Surface Morphology Study of Homogenous SiO_2 and Nanocomposite SiO_2 Thin Dielectric Layers Containing a Plane of AgNPs

A. *Homogeneous SiO_2 thin layers*

Surface morphology studies on the homogeneous plasma silica layers are presented in Figs. 2(a) and 2(b) for the two different surface areas, 100 µm² and 1 µm², respectively. As reported on the two images, the arithmetic surface roughness is very low, of only R_a = 0.31 nm. Moreover, it is the same regardless the scanned surface area. It means that the surface has regularly distributed, small sized peaks and valleys. There is a small increase in the quadratic surface roughness for the larger scanned area (Fig. 2(a)), pointing to the presence of a small number of higher peaks, as can be seen in the figure, which most likely represent a small surface dust contamination. The studied thermal silica layer on area of 1 µm² is shown in Fig. 2(c). The thermal silica layers are known for their very good structural arrangement of the Si-O_4 tetrahedra, and thus very small surface roughness. As shown in the image, it presents a bit lower, but similar values for the arithmetic and quadratic roughness, as for the plasma silica layer (Fig. 2(b)). This only confirms that the applied plasma deposition method offers a very good surface planarity of the obtained plasma silica layers. Comparison between arithmetic roughness of the thermal and plasma silica along a vertical line, presented in Fig. 2(d), supports the surface observations.

B. *Nanocomposite SiO_2 layers containing a plane of AgNPs, embedded at the layer sub-surface*

Nanostructures with different size and surface density of the AgNPs were elaborated for the current study. All studied here structures, the homogeneous SiO_2-layers presented in the previous section and the nanocomposites were elaborated with the same total thickness of the structures, d_{tot} = 135 nm. In order to evaluate the imposed waviness on the SiO_2-surface by different in size AgNPs, the latter were embedded in the silica layer at the same depth, d_c = 5 nm. The thickness of the SiO_2-cover layer was

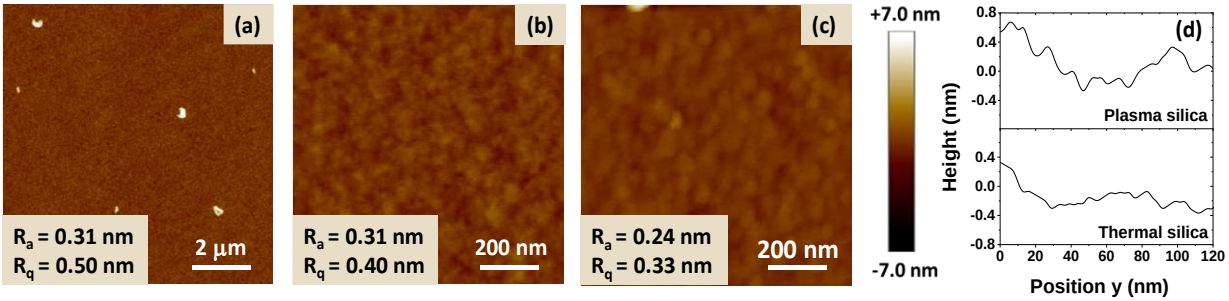

Figure 2. AFM morphology images of (a) and (b) plasma deposited SiO_2 layer for surfaces of 100 µm² and 1 µm², respectively, (c) thermal SiO_2 layer for surface of 1 µm² for comparison, and (d) upper part: surface roughness along a line from the plasma deposited silica layer, shown in panel (b) and lower part: the same but for the thermal silica, shown in panel (c).

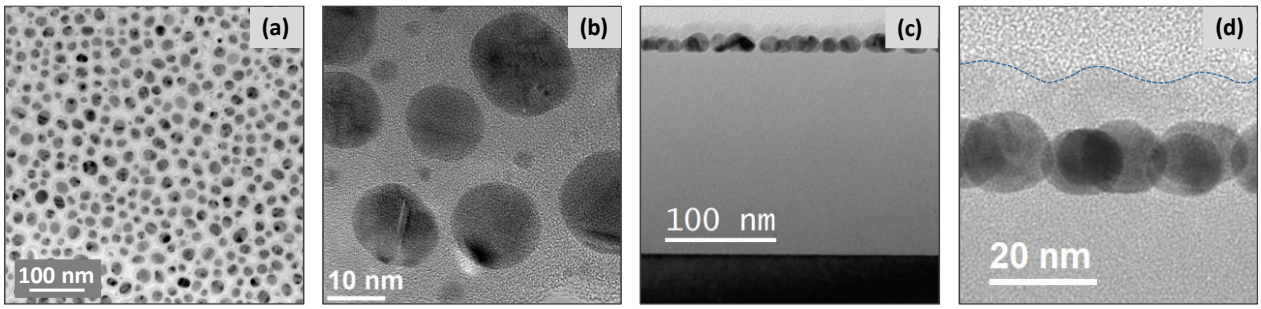

Figure 3. TEM images of the studied AgNPs-based nanocomposite structures containing large AgNPs: (a) top-view, (b) high-resolution image, (c) cross-section view of the complete structure and (d) cross-section view of the upper part of the structure.

obtained from ellipsometry measurements. Figure 3 shows TEM images of this stratified structure. According to the plan view image (Fig. 3(a)) after image processing one obtains for the AgNPs that they are of size of 17.8 ± 4.6 nm, density of 3.1×10^{11} NPs/cm^2 and spherical shape (eccentricity lower than 0.4). The AgNPs are polycrystalline, as shown in the high-resolution image (Fig. 3(b)) and some of them present complex structuring (twined or high order mixing). The cross-view image shows that the AgNPs are organized in a mono-layer, distributed in a plane (Fig. 3(c)) and are located very close to the SiO_2-surface. Since the plasma deposition is conformal to the surface morphology, one can see that the SiO_2-cover layer envelops the AgNPs and due to its small thickness *i.e.*, to the small depth at which the AgNPs are embedded, the surface of the structure presents a waviness, as underlined by the discontinuous blue line (Fig. 3(d)).

The study performed by AFM on the surface morphology of such AgNPs-based nanocomposite structures (Fig. 4) confirms the features underlined by the TEM observations. Figures 4(a) – (c) show the surface morphology for small AgNPs (size less than 10 nm), embedded in SiO_2-layer at 5 nm beneath the surface for surface area of 100 µm^2 (Fig. 4(a)) and 1 µm^2 (Fig. 4(b)). A comparison of these two scales shows that the higher resolution gives a higher arithmetic roughness and a higher quadratic roughness, where the former is easily understood in terms of resolution and the latter implies a regular structuring of the surface, *i.e.*, randomly distributed in the plane AgNPs of small distribution in size, in this case. The imposed by the AgNPs waviness of the surface can be seen in (Fig. 4(c)) for a line along y-direction (as presented in the insert of Fig. 4(b)) that covers three aligned AgNPs.

The same AFM surface morphology study was performed for large AgNPs (average size of 20 nm), synthesized under plasma conditions as for the AgNPs-structure presented in Fig. 3. The obtained results are shown in Fig. 4(d) – (f). The same trends, as those observed for the small AgNPs (4(a) – (c)) are found here, although a bit amplified. Both, the arithmetic and the quadratic roughness are almost doubled compared to the case of small AgNPs, and the quadratic roughness is again found higher for the

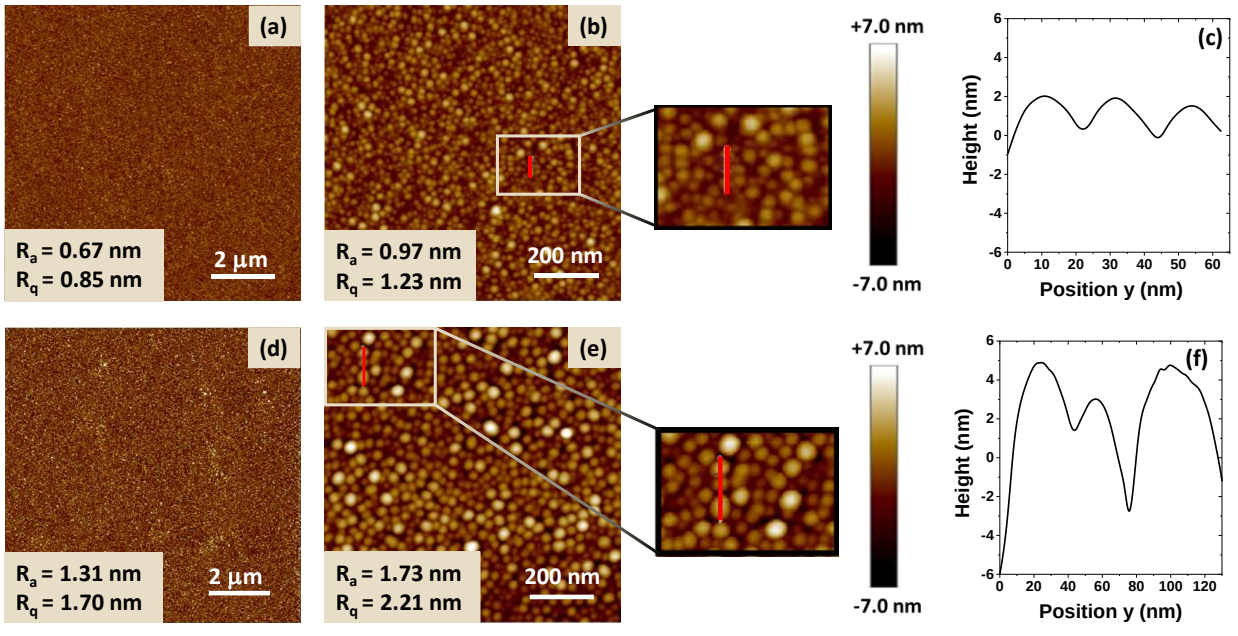

Figure 4. AFM morphology images of the AgNPs-based nanocomposite structures for nanoparticles embedded at 5 nm beneath the SiO_2 surface: (a)-(c) small AgNPs (< 10 nm in size), where (a) is for surface of 100 µm^2, (b) for 1 µm^2, and (c) shows the surface waviness along a line covering three AgNPs, (d) – (f) the same as for the corresponding (a) – (c) panels but reporting on large AgNPs (average size of 20 nm).

higher resolution study, thus emphasizing the random distribution of the AgNPs in the plane. The obtained higher values are mainly due to the higher dispersion in size of the large AgNPs, which can be clearly seen in Fig. 4(f) that traces a line over three AgNPs (presented in the insert of Fig. 4(e)).

The apparent average size of AgNPs in the structures was determined from the AFM surface morphology profiles as the Full Width at Half Maximum of the bumps. Statistic study on the bump widths was performed selecting 20 AgNPs bumps randomly distributed over the surface and the average AgNPs bump value and the corresponding dispersion were extracted. The obtained results are reported in Table I for three different cases: small AgNPs, medium AgNPs (AFM morphology not shown here) and large AgNPs. One can notice the conserved trend of increase of the bump width, as well as the increased dispersion with increasing the AgNPs average size found by the AFM surface morphology study. If subtracting the 5 nm thick cover layer from both sides around the AgNPs, as shown in Fig. 1, one finds that the apparent average size of the AgNPs in the plane concurs well with the AgNPs average size, as determined from other methods.

TABLE I. AVERAGE SIZE OF THE AGNPS AND AVERAGE WIDTH OF THE AGNPS-BUMPS FOR THE DIFFERENT SAMPLES

Sample	**AgNPs average size according to the plasma synthesis conditions**	**Width of the AgNPs bump considering the SiO_2-cover layer**
S1	< 10 nm	15 ± 3 nm
S2	12 nm	25 ± 4 nm
S3	20 nm	31 ± 7 nm

Looking on the surface waviness imposed by the embedded AgNPs and its increase with increasing the size of AgNPs one can realize that the electrical contacts, when taken on such surfaces, would be strongly impacted by this effect. When the electrodes are deposited on the sample surface there will be points of electric field enhancement solely due to the surface waviness. Brief assessment of the electric field for an applied potential of $V = +5$ V gives the following: the applied electric field will be of 3.7×10^7 V/m for the homogeneous SiO_2-layer. We recall here that all studied samples have the same total thickness, $d_{tot} = 135$ nm. Without accounting for the presence of AgNPs in the structure or for possible coupling between the AgNPs and the electrode, as previously reported [9], the distribution of the applied electric field in this tip-to-plane geometrical configuration can be calculated according to:

$$E = \frac{2V}{\left(R_t + 2z\right)\ln\left(2\,d_{tot}/R_t + 1\right)}, \qquad (2)$$

where V is the applied potential, R_t is the curvature radius of the tip-like structure, d_{tot} is the tip-to-plane distance and z is variable presenting the direction. Thus, the maximum electric field will be at the tip and there it will be enhanced by a factor of 20 (up to 7.4×10^8 V/m) compared to the homogeneous one, if considering curvature radius of $R_t = 3.0$ nm of the valley dips at positions 22 nm and 44 nm, for the small AgNPs (Fig. 4(c)) and by a factor of 35 (up to 1.3×10^9 V/m), when the curvature radius of the valley dip is $R_t = 1.5$ nm, as for the large AgNPs (at position 75 nm on Fig. 4(f)). Modifications of the designed electric field of the kind will strongly impact the device performance and shall be accounted for when taking electrical contacts to connect materials with such surface waviness with external circuitry.

IV. CONCLUSION

This work presents a study on the surface morphology of AgNPs-based nanocomposites performed by AFM. It shows that embedding AgNPs in a SiO_2-layer at small depths behind the surface imposes a waviness in the surface morphology. According to the obtained quadratic roughness at different resolutions, one can conclude that the AgNPs are randomly distributed in the plane and that their distribution in size is small. The obtained by AFM roughness profiles allow assessment of the electric field at the enhancement points between two adjacent AgNPs, imposed by the surface waviness. It is found that the electric field can be enhanced by a factor of 20 and more, which means that the applied electric field will strongly differ from the designed one. Further work is related to thorough structural analyses by TEM observations and measurements of charge injection and transport in such AgNPs-based nanocomposite structures.

ACKNOWLEDGMENT

The authors acknowledge support from the Centre de microcaractérisation Raymond Castaing (UAR 3623) of Université de Toulouse and thank Dr. A. Pugliara and Mr. L. Weingarten for the TEM observations.

REFERENCES

[1] G. M. Rebeiz, *RF MEMS: theory, design, and technology*. Hoboken, NJ: J. Wiley, 2003.

[2] J. Grollier, *et. al.*, « Neuromorphic spintronics », *Nat. Electron.*, vol.3, n°7, p.360-370, mars 2020, doi: 10.1038/s41928-019-0360-9.

[3] V. K. Sangwan and M. C. Hersam, « Neuromorphic nanoelectronic materials », *Nat. Nanotechnol.*, vol. 15, n° 7, p. 517-528, juill. 2020, doi: 10.1038/s41565-020-0647-z.

[4] C. Delacour and A. Todri-Sanial, « Mapping Hebbian Learning Rules to Coupling Resistances for Oscillatory Neural Networks », *Front. Neurosci.*, vol. 15, p. 694549, nov. 2021, doi: 10.3389/fnins.2021.694549.

[5] Y. Ren, *et al.*, « Highly sensitive and flexible strain sensor based on Au thin film », *J. Micromechanics Microengineering*, vol. 29, n° 1, p. 015001, janv. 2019, doi: 10.1088/1361-6439/aaebe4.

[6] R. He, *et al.*, « Flexible Miniaturized Sensor Technologies for Long-Term Physiological Monitoring », *Npj Flex. Electron.*, vol. 6, n° 1, p. 20, mars 2022, doi: 10.1038/s41528-022-00146-y.

[7] Z. Zheng *et al.*, « Ionic shape-morphing microrobotic end-effectors for environmentally adaptive targeting, releasing, and sampling », *Nat. Commun.*, vol. 12, n° 1, p. 411, janv. 2021, doi: 10.1038/s41467-020-20697-w.

[8] A. Allain, *et al.*, « Electrical contacts to two-dimensional semiconductors », *Nat. Mater.*, vol. 14, n° 12, p. 1195-1205, déc. 2015, doi: 10.1038/nmat4452.

[9] C. Djaou, C. Villeneuve-Faure, K. Makasheva, L. Boudou, and G. Teyssedre, « Analysis of the charging kinetics in silver nanoparticles-silica nanocomposite dielectrics at different temperatures », *Nano Express*, vol. 2, n° 4, p. 044001, déc. 2021, doi: 10.1088/2632-959X/ac3886.

[10] K. Makasheva *et al.*, « Dielectric Engineering of Nanostructured Layers to Control the Transport of Injected Charges in Thin Dielectrics », *IEEE Trans. Nanotechnol.*, vol. 15, n° 6, p. 839-848, nov. 2016, doi: 10.1109/TNANO.2016.2553179.